

# Dynamics and Mechanism of Flame Retardants in Polymer Matrixes: Experiment and Simulation

Donghwan Yoon,<sup>†,⊥</sup> Hyun Tae Jung,<sup>†,⊥</sup> Gyemin Kwon,<sup>†</sup> Yeoeun Yoon,<sup>†</sup> Minsoo Lee,<sup>‡</sup> Imhyuck Bae,<sup>‡</sup> Beom Jun Joo,<sup>‡</sup> Mansuk Kim,<sup>‡</sup> Sun Ae Lee,<sup>‡</sup> Jihye Lee,<sup>¶</sup> Yeonhee Lee,<sup>¶</sup> Eunseog Cho,<sup>§</sup> Kwanwoo Shin,<sup>\*,†</sup> and Bong June Sung<sup>\*,†</sup>

<sup>†</sup>Department of Chemistry and Institute for Biological Interfaces, Sogang University, Seoul 121-742, Republic of Korea

<sup>‡</sup>Chemical Synthesis Group, Samsung Cheil Industries, Uiwang 437-711, Republic of Korea

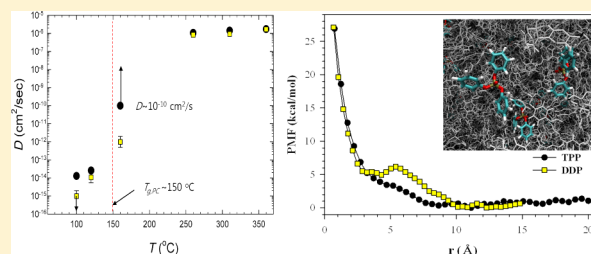
<sup>¶</sup>Advanced Analysis Center, Korea Institute of Science and Technology, Seoul 136-791, Republic of Korea

<sup>§</sup>Advanced Material Research Center, Samsung Advanced Institute of Technology, Samsung Electronics Company, 449-712 Republic of Korea

## Supporting Information

**ABSTRACT:** We investigate the dynamics and the mechanism of flame retardants in polycarbonate matrixes to explore for a way of designing efficient and environment-friendly flame retardants. The high phosphorus content of organic phosphates has been considered as a requirement for efficient flame retardants. We show, however, that one can enhance the efficiency of flame retardants even with a relatively low phosphorus content by tuning the dynamics and the intermolecular interactions of flame retardants. This would enable one to design bulkier flame retardants that should be less volatile and less harmful in indoor environments.

UL94 flammability tests indicate that even though the phosphorus content of 2,4-di-*tert*-butylphenyl diphenyl phosphate (DDP) is much smaller with two bulky tertiary butyl groups than that of triphenyl phosphate (TPP), DDP should be as efficient of a flame retardant as TPP, which is a widely used flame retardant. On the other hand, the 2-*tert*-butylphenyl diphenyl phosphate (2-*t*BuDP), with a lower phosphorus content than TPP but with a greater phosphorus content than DDP, is less efficient as a flame retardant than both DDP and TPP. Dynamic secondary ion mass spectrometry and molecular dynamics simulations reveal that the diffusion of DDP is slower by an order of magnitude at low temperature than that of TPP but becomes comparable to that of TPP at the ignition temperature. This implies that DDP should be much less volatile than TPP at low temperature, which is confirmed by thermogravimetric analysis. We also find from Fourier transform infrared spectroscopy that Fries rearrangement and char formation are suppressed more by DDP than by TPP. The low volatility and the suppressed char formation of DDP suggest that the enhanced flame retardancy of DDP should be attributed to its slow diffusivity at room temperature and yet sufficiently high diffusivity at high temperature.



## 1. INTRODUCTION

Flame retardants (FRs) are an important class of materials added to flammable polymer products in order to safeguard and promote human welfare.<sup>1–5</sup> Recently, due to tightened safety requirements, the importance of developing effective, yet environment-friendly FRs has grown in both industrial applications and scientific interest.<sup>6–9</sup> Health-hazardous halogen-based FRs are prohibited in many countries, and instead, various organic phosphorus-based compounds such as aryl phosphates are investigated.<sup>10–16</sup> Especially, triphenyl phosphate (TPP), resorcinol bis(diphenyl phosphate) (RDP), and bisphenol A bis(diphenyl phosphate) (BDP) have been studied extensively.<sup>17–19</sup> However, due to their high volatility, a significant amount of aryl phosphates are released from polymer products in indoor environments, often resulting in contact allergens and neurotoxins.<sup>20</sup> Therefore, designing less

volatile FRs but with high efficiency is still an issue of environmental importance.

Designing new FRs is a challenging task because flame retardancy mechanisms at a molecular level still remain elusive. In order to design a new FR, therefore, scientists often adhere to a simple guideline that FRs with a higher phosphorus content would perform better. For a given weight percentage of FRs in polymer matrixes, FRs with a lower phosphorus content generate a lower amount of phosphorus radicals. Then, more FRs should be inserted into polymer matrixes to secure sufficient phosphorus radicals, which may alter the physical properties of the polymer matrixes significantly.

Received: January 4, 2013

Revised: June 24, 2013

Published: June 24, 2013

According to the guideline, one may expect that TPP, a relatively small molecule but with a high phosphorus content, should be a good candidate for FRs. However, TPP is very volatile due to its relatively low molecular weight and may be released easily into indoor environments. In order to maintain the phosphorus content and reduce the volatility of TPPs, RDP and BDP are also used as FRs. However, mixing such FRs with polymers may lead to significant changes in physical properties of polymeric matrixes. We illustrate in this paper that one can improve the efficiency of FRs even with a relatively low phosphorus content by tuning the dynamics and the intermolecular interactions of FRs. We introduce bulky tertiary butyl groups to TPPs and synthesize 2,4-di-*tert*-butylphenyl diphenyl phosphate (DDP). The phosphorus content of DDP is smaller by about 25% than that of TPP. We find from flame tests and dynamic secondary ion mass spectrometry (DSIMS) that DDP is as efficient as TPP but much less volatile at low temperature.

There are two general mechanisms of organic based FRs, a gas-phase mechanism and a condensed-phase mechanism. Phosphorus-containing FRs usually employ both mechanisms.<sup>11,17,21,22</sup> Although one mechanism may dominate over the other depending on polymer types and FRs, the mechanism is often complicated. Highly volatile TPPs are active in the vapor phase and capture  $\text{H}^\bullet$  and  $\text{OH}^\bullet$  radicals, while oligomeric phosphate such as RDP and BDP with lower volatility are more active in the condensed phase, providing thermally stable char layers.<sup>23</sup> In the condensed-phase mechanism, FRs react with polymers such as polycarbonate (PC) and form char, which acts as a thermal insulator and protects underlying polymers. Murashko et al. suggested that PCs underwent Fries rearrangement and that aryl phosphate was trans-esterified with phenolic groups produced from PC,<sup>24</sup> thus forming char via thermal decomposition. Recently, the combination of volatile (i.e., TPP) and nonvolatile phosphates (i.e., RDP, or BDP) was found to be more effective than each additive taken alone,<sup>23,25,26</sup> indicating that the optimized volatility of FRs was one of critical factors to determine the effectiveness.

In this paper, we show from UL94 flame tests that DDP with additional tertiary butyl groups is as efficient in a PC matrix as TPP even though the phosphorus content of DDP is much smaller. However, the 2-*tert*-butylphenyl diphenyl phosphate (2-*t*BuDP) is less efficient as a FR than both DDP and TPP. We found from DSIMS and molecular dynamics (MD) simulations that the diffusion of DDP is slower by an order of magnitude at low temperature than that of TPP, but the diffusion coefficient of DDP becomes comparable to that of TPP at the ignition temperature. This is consistent with results from thermogravimetric analysis (TGA) that DDP is less volatile compared to TPP below the ignition temperature. This implies that DDPs would be released to a lesser extent and could be less harmful in indoor environments. Interestingly, Fourier transform infrared spectroscopy (FTIR) experiments suggest that DDP should be less likely to form char in PCs because Fries rearrangement is suppressed by DDP, and the computation of the potential of mean force (PMF) between a FR and a PC chain shows that the tertiary butyl functional group should impose a thermal energy barrier of about 7 kcal/mol, which supports the results from FTIR experiments. The improved flame retardancy of DDP can be attributed to our observations that a larger quantity of DDPs are reserved in polymer matrixes due to slow diffusion at low temperature, and the diffusivity of DDPs is enhanced at high temperature. This

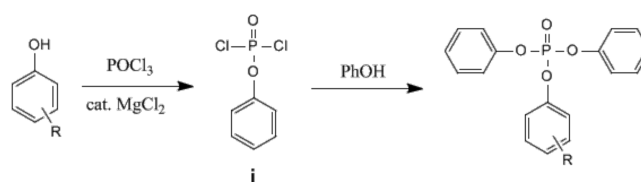
study on the dynamics and the mechanism of a new FR illustrates how one can improve the flame retardancy by tuning the dynamics and the intermolecular interactions of FRs.

This paper is organized as follows. The experimental and simulation methods are described in section 2, results and discussions are presented and discussed in section 3, and a summary and conclusions are presented in section 4.

## 2. EXPERIMENTAL AND SIMULATION METHODS

**2.1. Experimental Methods. Materials.** PC ( $M_w = 27\,072$ ) and TPP were obtained from Samsung Cheil Industries Inc. 2-*t*BuDP and DDP were synthesized using a following method.<sup>27</sup> When  $\text{POCl}_3$  was treated with ortho-substituted phenol in the presence of  $\text{MgCl}_2$  under toluene reflux, aryl dichlorophosphate (**i**) was formed exclusively. Remaining Cl atoms were allowed to react with phenol (PhOH) to furnish the desired phosphates (2-*t*BuDP and DDP) in high yields (Scheme 1). The chemical structures and the characteristics of

Scheme 1. Synthesis Scheme for FRs<sup>a</sup>



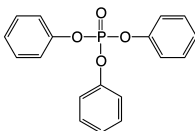
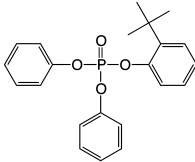
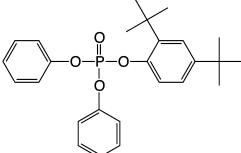
<sup>a</sup>As more tertiary butyl groups are introduced from TPP to 2-*t*BuDP to DDP, the phosphorous content of the FRs decreases.

FRs used in this study are summarized in Scheme 1 and Table 1. For 2-*t*BuDP, a hydrogen atom of TPP is substituted by a tertiary butyl group, and in the case of DDP, one more hydrogen atom needs be substituted by a tertiary butyl group. Therefore, the phosphorus content of FRs decreases significantly from TPP to 2-*t*BuDP to DDP.

We employ UL94, a common flammability test for polymeric materials, to investigate the flame retardancy of TPP, 2-*t*BuDP, and DDP. All three FRs of 5 wt % were compounded with PCs. All specimens were 3.2 mm thick after extrusion. When compounding with PCs, we also added a lubricant and an antidripping agent (Teflon), of which the concentrations were 0.3 and 0.5 wt %, respectively. We measured times taken for the first and the second combustion of the specimens and repeated the measurements five times.

DSIMS was used to determine the tracer diffusion coefficient ( $D$ ) of FRs as a function of temperature because DSIMS could trace phosphorus ions in a PC matrix. Bilayers on a silicon wafer were prepared as follows: thin films of PC were spun-cast directly onto silicon wafers from chloroform solution. The thickness of this layer was about 300 nm. Another PC layer containing 20 wt % FRs (TPP or DDP) was spun-cast onto a glass slide and floated from DI water onto the PC layer, producing a bilayered film with the FR/PC layer on the PC layer. The bilayer samples were then annealed for different times at desired temperatures from 100 to 200 °C in a vacuum of  $10^{-4}$  Torr. After annealing, all samples were covered with an approximately 50 nm thick sacrificial layer of deuterated polystyrene ( $d_{10}$ PS). After the exact thickness was determined by X-ray reflectivity, this sacrificial layer was used to determine the exact thicknesses of the layers used. Each sample was individually measured by DSIMS using either a Cameca IMS-4FE7 secondary ion mass spectrometer or a ion TOF V time-

Table 1. FRs Used in This Study<sup>a</sup>

Compound	Structure	R	T <sub>id</sub>	UL94
TPP		H	206	V-0
2-tBuDP		2-tBu	218	V-1
DDP		2,4-tBu	235	V-0

<sup>a</sup>The initial decomposition temperature was measured by using thermogravimetry under air at 5% weight loss.

of-flight SIMS instrument at the Advanced Analysis Center of the Korea Institute of Science and Technology (KIST, Korea). Intensities of emitted negative ions ( $\text{H}^-$ ,  $\text{D}^-$ ,  $\text{C}^-$ ,  $\text{CH}^-$ ,  $\text{CD}^-$ ,  $\text{O}^-$ ,  $\text{Si}^-$ ,  $\text{P}^-$ ,  $\text{PO}^-$ ,  $\text{PO}_2^-$ , and  $\text{PO}_3^-$ ) were simultaneously monitored. In the Cameca IMS-4FE7, DSIMS was performed by bombarding the sample with a 6.0 KeV  $\text{Cs}^+$  ion beam. According to Fick's law, one can derive the density profiles ( $\phi(x)$ ) of  $\text{P}^-$  ions as a function of distance from the interface at time  $t$ , that is,

$$\phi(x) = \frac{1}{2} \left[ \text{erf} \left( \frac{h-x}{\sqrt{4Dt}} \right) + \text{erf} \left( \frac{h+x}{\sqrt{4Dt}} \right) \right] \quad (1)$$

where  $x$  is the distance from the interface, erf is an error function, and  $h$  is the thickness of a thin film. The  $\phi(x)$ 's overlap well with our DSIMS measurements. Values of  $D$  are obtained by fitting  $\phi(x)$  to measurements. Note that we have fixed the total concentration of the FRs for all samples to be 20 wt % and numerically processed the area of the obtained intensity profile of  $\text{P}^-$  (as shown in Figure S1(a) in the Supporting Information) to be a total of 20%.

TGA was carried out using a TGA 2050 thermogravimetric analyzer (TA Instruments) at a series of heating rates (2, 10, 20, and 30 °C  $\text{min}^{-1}$ ) in flowing nitrogen (100  $\text{cm}^3\text{min}^{-1}$ ) at temperatures from 30 to 700 °C. PC and PC with 10 wt % FRs were dissolved in chloroform first. The solvent was then evaporated at 70 °C in an oven.

FTIR was conducted by using a Cary 640 infrared spectrometer (Agilent Technologies). All measurements were performed by ATR mode with a ZnSe crystal. Solid residues of thermally degraded PC and FR/PC nanocomposites were collected from TGA, interrupted at various temperatures.

**2.2. Simulation Methods.** Configurations of mixtures of PCs and FRs (DDP or TPP) are constructed by using an amorphous cell.<sup>28</sup> Up to 28 PC chains and 4 or 8 FRs are placed in a simulation cell with periodic boundary conditions in all directions. Each PC chain consists of 8 or 16 monomer units, and the concentrations of FRs are fixed at 3 wt %. Molecules are placed initially in a sufficiently large simulation cell with a low density of 0.1  $\text{g}/\text{cm}^3$  in order to prevent phenyl rings of PCs from being catenated. We perform MD

simulations at a constant pressure of 1 GPa and temperature of 560 °C and increase the system density to 1  $\text{g}/\text{cm}^3$ . MD simulations are performed by using the COMPASS force field<sup>29–32</sup> and the Discover package in Materials Studio. In the simulations, the time step is 1 fs, and a cutoff distance for nonbonded interactions is 6.5 Å. Note that at the cutoff distance of 6.5 Å, the value of the potential energy is about 12% of the potential depth of the nonbonding interactions. The simulation cell dimensions range from 4.2 to 5.8 nm depending on the systems.

Systems are annealed at 2500 K by running additional MD simulations for 10 ps at constant volume. The configurations of the annealed systems are equilibrated at 260, 310, and 360 °C for 20 ns via NVT MD simulations. The average pressures of our NVT MD simulations are  $-0.09 \pm 0.1$ ,  $-0.06 \pm 0.11$ , and  $-0.04 \pm 0.1$  GPa for 260, 310, and 360 °C, respectively. Negative values of pressure usually indicate that the volume of the system tends to decrease and the volume of our systems may be large for a given temperature. However, in this study, we intend to simulate systems with a density of 1  $\text{g}/\text{cm}^3$  as in the experiments and to keep the volume constant. The negative pressure may be also attributed to the relatively short cutoff distance used in our simulations, which was chosen to reduce otherwise tremendous simulations times. We obtain at least two independent initial configurations for each condition and run MD simulations for up to 60 ns. The diffusion coefficients ( $D$ ) of DDP and TPP are calculated as follows

$$D = \lim_{t \rightarrow \infty} \frac{\langle (\vec{r}(t) - \vec{r}(t=0))^2 \rangle}{6t} \quad (2)$$

where  $\langle \dots \rangle$  denotes the ensemble average and  $\vec{r}(t)$  is the position vector of the center of mass of a FR at time  $t$ .

Intermolecular interaction between a polymer and a FR plays a critical role in determining the dynamics and the reactions of FRs. Therefore, we calculate the PMF between a PC chain and a FR by using the NAMD package<sup>33</sup> with the CHARMM27r force field<sup>34</sup> and Whitney and Yaris model.<sup>35</sup> The atomic charges of FRs and PC monomer units are obtained via a Mulliken population analysis and electronic structure calculations at the level of HF/6-31G(d). Initial configurations are

equilibrated for 20 ns at 370 °C with a Langevin thermostat. Then, we employ an umbrella sampling method with a biased harmonic potential and a weighted histogram analysis method (WHAM) to obtain PMFs. The biased harmonic potential is defined as follows

$$E_{\text{biased}} = \frac{K_f}{2}(d - d_r)^2 \quad (3)$$

where  $d$  is the distance between the center of mass of a FR and the center of the fourth and the fifth monomers of a PC chain and  $K_f$  is 20 kcal/mol/Å<sup>2</sup>. The value of  $d_r$  changes from 0.5 to 20.25 Å in increments of 0.25 Å. Each value corresponds to a sampling window. For each sampling window, systems are equilibrated for 100 ps and sampled for 1900 ps. In the PMF calculations, other PC chains are still present in the systems in addition to the PC chain with the biased harmonic potential imposed on it. In this study, different sets of force fields are used: the COMPASS force field for diffusion coefficients and the CHARMM27r force field for the PMF. Therefore, there should be certain differences in configurations of polymers and FRs between two different sets of simulations, but values of pressure estimated by two different force fields fluctuate within the same range in our systems. Also, note that a fair comparison is made between two different FRs; the identical force field is employed to calculate the same type of physical property of two different FRs.

### 3. RESULTS AND DISCUSSION

A generally accepted guideline to design FRs is that flame retardation efficiency improves with an increase in the phosphorus content of FRs. According to the guideline, the efficiency would deteriorate as we introduce bulky tertiary butyl groups to TPP. In UL94 experiments, we measured times taken for the first and the second combustion of five specimens of each FR. The average times taken for the first combustion of TPP and DDP were  $1.4 \pm 2.0$  and  $1.0 \pm 0.6$  s, respectively, which were much shorter than that of 2-*t*BuDP ( $6.2 \pm 1.4$  s). Times for the second combustion of TPP ( $5.4 \pm 2.6$  s) and DDP ( $3.1 \pm 1.7$  s) were still shorter than that ( $10.3 \pm 2.0$  s) of 2-*t*BuDP (as shown in Table S1 in the Supporting Information). The errors are one standard deviation of measured times. Therefore, TPP and DDP in PC matrixes are classified as V-0, while 2-*t*BuDP is classified as V-1, that is, DDP is as efficient as TPP even though the efficiency of 2-*t*BuDP deteriorates. This suggests that the bulky tertiary butyl groups should play a certain role other than simply decreasing the phosphorus content. Studies on how tertiary butyl groups would affect the dynamics and intermolecular interactions of FRs would help understand the flame retardancy mechanism at a molecular level.

We investigate the effects of bulky tertiary butyl groups on the dynamics of FRs in PC matrixes by employing DSIMS.<sup>36,37</sup> In Figure 1a are the density profiles ( $\phi(x)$ ) of P<sup>−</sup> ions as a function of distance from the interface at  $t = 1$  min for both as-spun and annealed samples. As one can see in Figure 1a (measured at 160 °C) and Figure S1(b) (Supporting Information) (measured at 120 °C), asymmetric diffusions into a bulk PC layer were seen, and  $D$  was a single fitting parameter to fit three different spectra, obtained at various times (see, Figure S1(b), Supporting Information). Diffusion coefficients of DDP are much smaller by up to an order of magnitude than those of TPP at 100 and 120 °C (Figure 1b). Near or above  $T_g$  ( $\sim 150$  °C) of PC, TPPs diffuse significantly

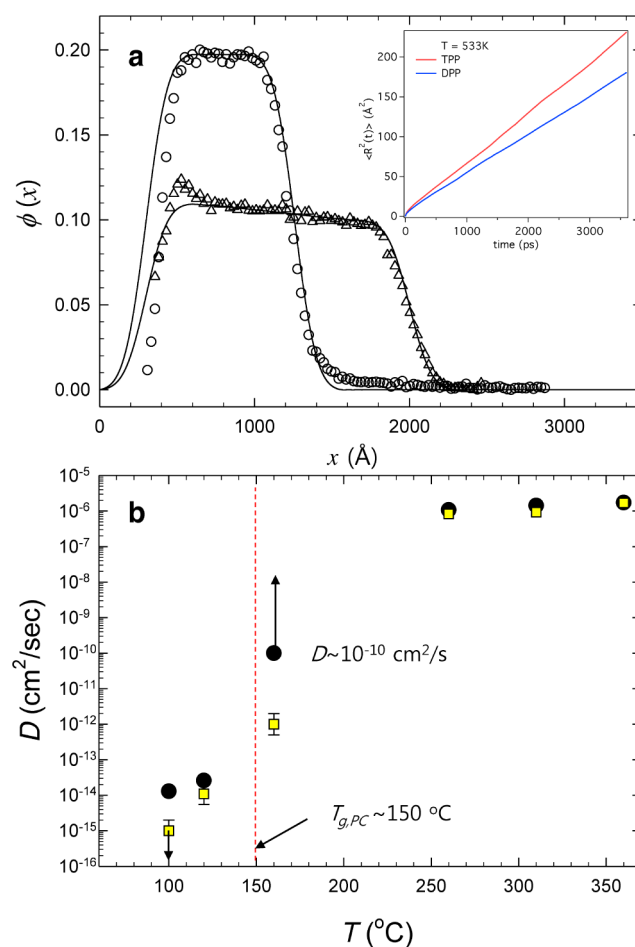


**Figure 1.** (a) DSIMS measurements of density profiles of P<sup>−</sup> ions of a PC/DDP nanocomposite for as-spun (O) and annealed samples at 160 °C for 1 min (Δ). Solid lines are fits to DSIMS measurements. In the inset is the simulation results for the mean-square displacement ( $R^2(t)$ ) for DDP and TPP at 260 °C. (b) Experimental and simulation results for diffusion coefficients ( $D$ ) of TPP and DDP as a function of  $T$ . Circles and squares represent TPP and DDP, respectively. Note that values of  $D$ 's at high  $T$  ( $>200$  °C) are estimated from MD simulations. Values of  $D$ 's at low  $T$  ( $<200$  °C) are obtained by fitting  $\phi(x)$  to DSIMS measurements. A vertical dotted line represents  $T_g = 150$  °C of PC. Two solid arrows indicate that two data points are outside of the experimental limit for  $D$ .

fast, and their diffusion coefficients exceed our experimental limit (about  $1.00 \times 10^{-10}$  cm<sup>2</sup>/s). Meanwhile, the diffusion of DDP is still much lower than that of TPP around  $T_g$ .

The diffusion coefficients of TPP and DDP at high temperature are estimated by using MD simulations. Diffusion coefficients at temperatures higher than 200 °C cannot be estimated by using DSIMS because the diffusion coefficient exceeds the measurement limit of DSIMS. However, the mobility (or the volatility) of FRs at the processing temperature and the ignition temperature should relate closely to the efficiency of FRs. Therefore, MD simulations are conducted at specific temperatures, such as the processing temperature (260 °C) of a commercial PC product and ignition temperature (360 °C). Even at such high temperatures, TPP diffuses generally faster than DDP. (Figure 1b) However, at the ignition temperature (360 °C),  $D$  of DDP increases to about  $1.69 \times 10^{-6}$  cm<sup>2</sup>/s, becoming almost comparable to that of TPP. Because the monophosphate FRs, which are active in the vapor



phase, need to volatilize to form active radicals at the ignition point, the enhanced diffusion of DDP at the ignition temperature might be one of the reasons for its high efficiency as a FR. However, note that the simulated values of  $D$ 's would deviate from true  $D$  values for FRs in PCs. Even though the COMPASS force field and MD simulations have been employed extensively to predict dynamic properties, it should be still a formidable task predicting quantitatively accurate diffusion coefficients. Also, the degree of polymerization of PCs is also small in simulations even though we consider that some PC chains might be decomposed into small fragments at high temperatures due to high thermal energy.

TGA also shows that DDP is much less volatile in PCs at relatively low temperatures than TPP. The TGA curves of PC, TPP/PC, and DDP/PC at a ramp rate of 2 °C/min are shown in Figure 2. In comparison with degradation of virgin PC, the

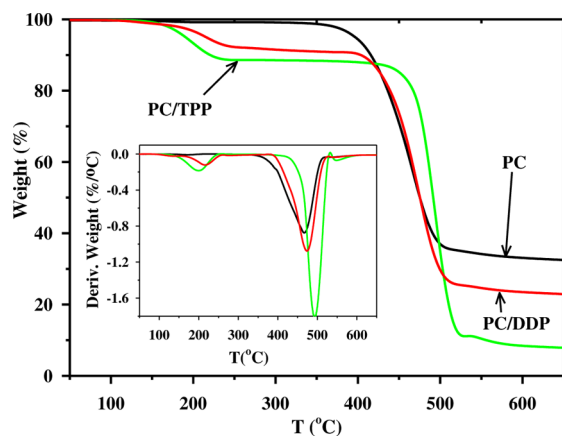


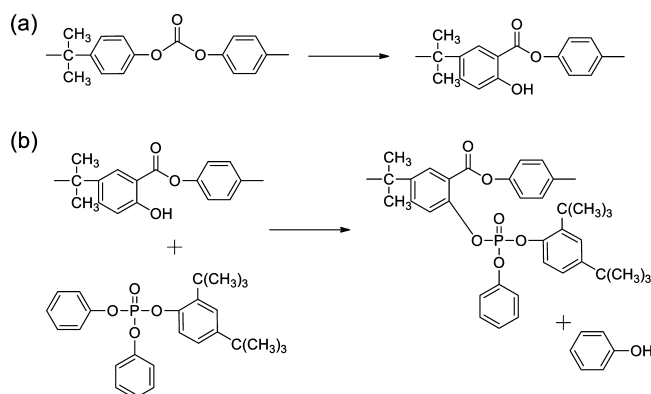
**Figure 2.** TGA curves: PC (black), TPP/PC mixture (green), and DDP/PC mixture (red). In the inset are the derivatives of weight loss in terms of temperature.

weight loss of TPP/PC and DDP/PC begin at lower temperature, indicative of the vaporization of FRs. Furthermore, the TGA curve indicates that TPP is more volatile than DDP. The volatile FR would then interact with PC, either by inhibiting the formation of free radicals in the main chain PC as a radical scavenger or by promoting cross-linking of the PC chains (via trans-esterification). The thermal stability of PC is improved due to FRs such that the maximum values of the derivative of weight loss shift to higher temperatures, as depicted in the inset of Figure 2.

To clarify the influence of the FR on thermal decomposition behaviors, we have added the series of TGA curves in Figure S2 (Supporting Information) measured at different heating rates: 2, 10, 20, and 30 K/min. Using the Kissinger method,<sup>38</sup> which is the numerical relation between the reciprocal of the temperature and the logarithm of the heating rate (the slopes in Figure S2(d), Supporting Information), the energies of activation,  $E_a$ , on thermal degradation of each sample were successfully obtained. The values of  $E_a$  for PC, TPP/PC, and DDP/PC were  $181 \pm 5$ ,  $235 \pm 5$ , and  $207 \pm 5$  kJ/mol, respectively. These results indicate that (1) DDP in fact reinforces its polymer matrix from the thermal decomposition and (2) TPP is more effective in the char-forming mechanism than DDP. The lower-energy barrier of thermal degradation of DDP/PC is probably due to the presence of tertiary butyl groups, which hinders the cross-linking of the polymer matrix upon the incorporation of the FR into the polymer matrix.

In order to understand how tertiary butyl groups would influence flame retardancy mechanisms, especially the char formation, we perform FTIR experiments for TPP/PC and DDP/PC mixtures at different mass loss stages of TGA curves. PCs decompose via several processes.<sup>39–41</sup> In particular, phenolic groups are generated via Fries rearrangement of carbonate linkages.<sup>24</sup> Then, phenolic groups react with FRs via trans-esterification, thus creating a cross-linked structure (Scheme 2). The cross-linked structure should be responsible for the char formation that is a key step for the condensed-phase mechanism.

**Scheme 2.** (a) Fries Rearrangement and (B) Trans-Esterification of PCs



We monitor the formation of phenolic groups (Figure 3) and the extinction of carbonate linkages (Figure 4) at different mass loss stages. For TPP/PC mixtures, peaks at  $3487\text{--}3533\text{ cm}^{-1}$ , which correspond to phenol O–H, develop at 31% mass loss, whereas for DDP/PC mixtures, it is not until 60% mass loss that such peaks appear, as shown in Figure 3. This suggests that the generation of the phenolic group is deferred in DDP/PC

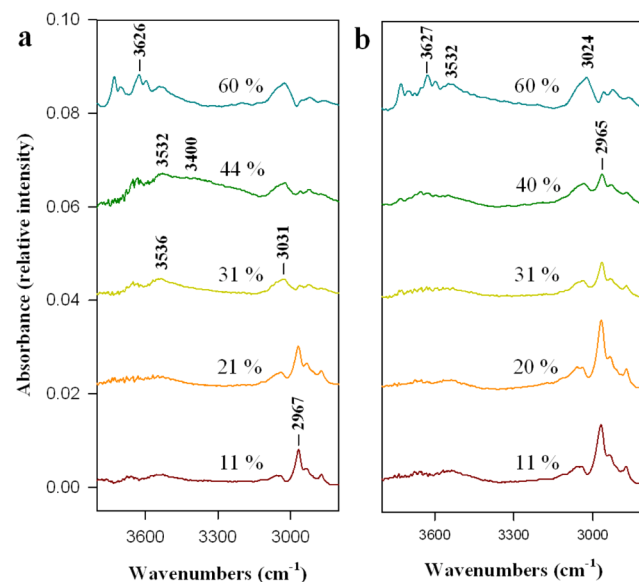


**Figure 3.** Infrared spectra of (a) TPP/PC and (b) DDP/PC composites at each mass loss stage from 3800 to 2800  $\text{cm}^{-1}$ . Peaks at  $3487\text{--}3533\text{ cm}^{-1}$  develop at 31% mass loss for TPP/PC mixtures. However, such peaks appear only at 60% mass loss for DDP/PC mixtures.

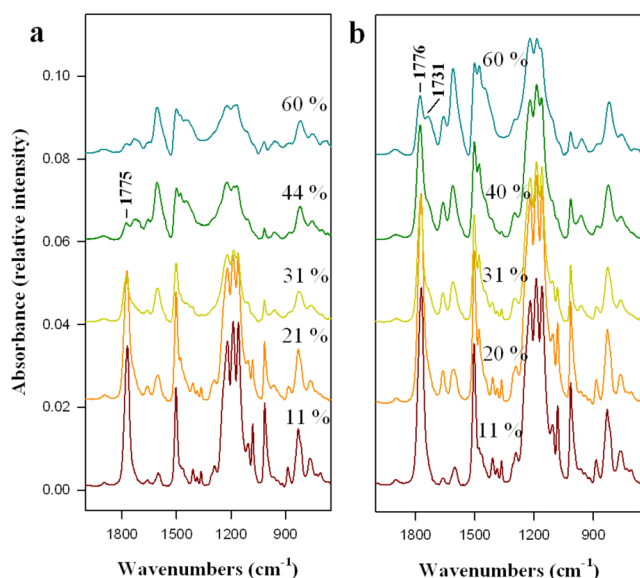


**Figure 4.** Infrared spectra of (a) TPP/PC and (b) DDP/PC composites at each mass loss stage from 2000 to 650  $\text{cm}^{-1}$ . The peak at 1775  $\text{cm}^{-1}$  disappears at 44% mass loss for TPP/PC mixtures. However, the peak remains until 60% mass loss for DDP/PC mixtures.

mixtures compared to that in TPP/PC mixtures. Similarly, a peak at 1775  $\text{cm}^{-1}$ , which corresponds to the C=O stretch of a carbonate linkage, disappears at 44% mass loss for TPP/PC mixtures. However, for DDP/PC mixtures, the peak does not disappear even for 60% mass loss (Figure 4). These results imply that DDP should stabilize the carbonate linkage and inhibit Fries rearrangement. The char formation is suppressed with DDP compared to that with TPP. Moreover, for TPPs, the gas-phase mechanism is dominant,<sup>4</sup> from which we suggest that for DDPs, the gas-phase mechanism would dominate over the condensed-phase mechanism.

The PMF between a PC and a FR is studied by performing molecular simulations. It may provide key information regarding the intermolecular interaction averaged over all configurations of all FRs in the polymer PC matrix. As depicted in Figure 5, an additional energy barrier of about 7 kcal/mol

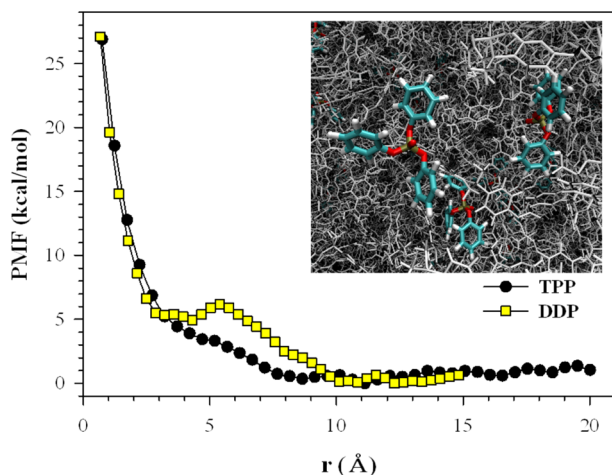


**Figure 5.** Simulation results for the PMF for DDP and TPP in PC matrixes. The abscissa is the distance ( $r$ ) between the center of mass of FRs and the center of the fourth and fifth monomers of a PC chain. In the inset is a representative snapshot of simulations.

appears when DDP approaches a PC chain with distance of  $\sim 6$  Å. Such an energy barrier is not observed for TPPs. Because of the energy barrier, it would be more difficult for phenolic OH groups of rearranged PCs to react with DDPs than with TPPs. This calculation is, therefore, supportive of our inference drawn from FTIR experiments that the char formation and the transesterification would be rendered less efficient and the condensed-phase mechanism should be suppressed for DDPs compared to TPPs.

#### 4. SUMMARY AND CONCLUSIONS

We investigate a newly synthesized FR, DDP, and find from UL94 flame tests that DDP with a relatively low phosphorus content is as efficient as TPP, which is widely used in industry. We also find that the 2-*t*BuDP, with a less phosphorus content than TPP but with a more phosphorus content than DDP, is less efficient than DDP and TPP. This is contrary to the generally accepted notion that FRs with a high phosphorus content should perform more efficiently. We discover from DSIMS experiments, TGA, and MD simulations that DDP is less volatile at low temperature and is sufficiently mobile at the ignition temperature. This helps a large amount of DDPs to remain in samples, which should be the reason for the high efficiency of DDP. Also, such low volatility of DDP also makes DDP a good candidate for environment-friendly FRs.

We also find from FTIR experiments that Fries rearrangement and trans-esterification are suppressed with DDP in PC matrixes compared to TPP, which is underpinned by our PMF calculations. Considering that TPPs are active in the vapor phase and the gas-phase mechanism is a dominant one for TPPs, the gas-phase mechanism should also dominate over the condensed-phase mechanism for DDPs.

In this work, we illustrate how one can tune the dynamics and the intermolecular interaction of FRs by introducing simple functional groups and that changes in the dynamics and the intermolecular interactions may improve the efficiency of FRs. We believe that such a strategy could be applied to design more efficient and environment-friendly FRs in future research.

#### ■ ASSOCIATED CONTENT

##### Supporting Information

Additional data and fits for DSIMS, TGA, and MD simulations are provided. This material is available free of charge via the Internet at <http://pubs.acs.org>.

#### ■ AUTHOR INFORMATION

##### Corresponding Author

\*E-mail: kwshin@sogang.ac.kr (K.S.); bjsung@sogang.ac.kr (B.J.S.).

##### Author Contributions

The manuscript was written through contributions of all authors. All authors have given approval to the final version of the manuscript.

##### Author Contributions

<sup>†</sup>D.Y. and H.T.J. contributed equally.

##### Notes

The authors declare no competing financial interest.

#### ■ ACKNOWLEDGMENTS

This work was supported by the National Research Foundation of Korea (NRF) under Grant No. NRF-2011-220-C00030. We acknowledge the financial support from the Ministry of

Education, Science and Technology, subjected to the project EDISON (EDucation-research Integration through Simulation On the Net, Grant No.: 2012M3C1A6035363). This research was supported by Advanced Research Center for Nuclear Excellence funded by MEST, Korea.

## REFERENCES

- (1) Granzow, A. Flame Retardation by Phosphorus Compounds. *Acc. Chem. Res.* **1978**, *11*, 177–183.
- (2) Sjödin, A.; Carlsson, H.; Thuresson, K.; Sjölin, S.; Bergman, A.; Ostman, C. Flame Retardants in Indoor Air at an Electronics Recycling Plant and at Other Work Environments. *Environ. Sci. Technol.* **2001**, *35*, 448–454.
- (3) Nyden, M. R.; Forney, G. P.; Brown, J. E. Molecular Modeling of Polymer Flammability: Application to the Design of Flame-Resistant Polyethylene. *Macromolecules* **1992**, *25*, 1658–1666.
- (4) Morgan, A. B.; Wilkie, C. A. *Flame Retardant Polymer Nanocomposites*; John Wiley & Sons, Inc.: New York, 2007.
- (5) Yu, H.; Liu, J.; Wang, Z.; Jiang, Z.; Tang, T. Combination of Carbon Nanotubes with  $\text{Ni}_2\text{O}_3$  for Simultaneously Improving the Flame Retardancy and Mechanical Properties of Polyethylene. *J. Phys. Chem. C* **2009**, *113*, 13092–13097.
- (6) Hale, R. C.; Guardia, M. J. L.; Harvey, E. P.; Gaylor, M. O.; Mainor, T. M.; Duff, W. H. Flame Retardants: Persistent Pollutants in Land-Applied Sludges. *Nature* **2001**, *412*, 140–141.
- (7) Morgan, A. B.; Tour, J. M. Synthesis and Testing of Nonhalogenated Alkyne-Containing Flame-Retarding Polymer Additives. *Macromolecules* **1998**, *31*, 2857–2865.
- (8) Morf, L. S.; Tremp, J.; Gloor, R.; Huber, Y.; Stengele, M.; Zennegg, M. Brominated Flame Retardants in Waste Electrical and Electronic Equipment: Substance Flows in a Recycling Plant. *Environ. Sci. Technol.* **2005**, *39*, 8691–8699.
- (9) Ranganathan, T.; Zilberman, J.; Farris, R. J.; Coughlin, E. B.; Emrick, T. Synthesis and Characterization of Halogen-Free Antiflamable Polyphosphonates Containing 4,4'-Bishydroxydeoxybenzoin. *Macromolecules* **2006**, *39*, 5974–5975.
- (10) Laoutid, F.; Bonnaud, L.; Alexandre, M.; Lopez-Cuesta, J. M.; Dubois, P. New Prospects in Flame Retardant Polymer Materials: From Fundamentals to Nanocomposites. *Mater. Sci. Eng. Res.* **2009**, *63*, 100–125.
- (11) Pawlowski, K. H.; Scharrel, B. Flame Retardancy Mechanisms of Triphenyl Phosphate, Resorcinol Bis(diphenyl phosphate) and Bisphenol A Bis(diphenyl phosphate) in Polycarbonate/acrylonitrile–Butadiene–Styrene Blends. *Polym. Int.* **2007**, *56*, 1404–1414.
- (12) Jang, B. N.; Wilkie, C. A. The Effects of Triphenylphosphate and Resorcinol-bis(diphenylphosphate) on the Thermal Degradation of Polycarbonate in Air. *Thermochim. Acta* **2005**, *433*, 1–12.
- (13) Marklund, A.; Andersson, B.; Haglund, P. Screening of Organophosphorus Compounds and Their Distribution in Various Indoor Environments. *Chemosphere* **2003**, *53*, 1137–1146.
- (14) Andresen, J. A.; Grundmann, A.; Bester, K. Organophosphorus Flame Retardants and Plasticizers in Surface Waters. *Sci. Total Environ.* **2004**, *332*, 155–166.
- (15) Carlsson, H.; Nilsson, U.; Becker, G.; Östman, C. Organophosphate Ester Flame Retardants and Plasticizers in the Indoor Environment: Analytical Methodology and Occurrence. *Environ. Sci. Technol.* **1997**, *31*, 2931–2936.
- (16) Marklund, A.; Andersson, B.; Haglund, P. Organophosphorus Flame Retardants and Plasticizers in Air from Various Indoor Environments. *J. Environ. Monit.* **2005**, *7*, 814–819.
- (17) Levchik, S. V.; Weil, E. D. A Review of Recent Progress in Phosphorus-Based Flame Retardants. *J. Fire Sci.* **2006**, *24*, 345–364.
- (18) Pack, S.; Kashiwagi, T.; Cao, C.; Korach, C. S.; Lewin, M.; Rafailovich, M. H. Role of Surface Interactions in the Synergizing Polymer/Clay Flame Retardant Properties. *Macromolecules* **2010**, *43*, 5338–5351.
- (19) Carlson, H.; Nilsson, U.; Östman, C. Video Display Units: An Emission Source of the Contact Allergenic Flame Retardant Triphenyl Phosphate in the Indoor Environment. *Environ. Sci. Technol.* **2000**, *34*, 3885–3889.
- (20) Nobile, E. R.; Page, S. W.; Lombardo, P. Characterization of Four Commercial Flame Retardant Aryl Phosphates. *Bull. Environ. Contam. Toxicol.* **1980**, *25*, 755–761.
- (21) Hastie, J. W.; McBee, C. L. Mechanistic Studies of Triphenylphosphine Oxide–Poly(ethyleneterephthalate) and Related Flame Retardant Systems. *Natl. Bur. Stand., [Tech. Rep.] NBISR (U.S.)* **1975**, *75–741*, 1–43.
- (22) Green, J. A. Phosphorus–Bromine Flame Retardant for Engineering Thermoplastics—A Review. *J. Fire Sci.* **1994**, *12*, 388–408.
- (23) Levchik, S. V.; Weil, E. D. Overview of Recent Developments in the Flame Retardancy of Polycarbonates. *Polym. Int.* **2005**, *54*, 981–998.
- (24) Murashko, E. A.; Levchik, G. F.; Levchik, S. V.; Bright, D. A.; Dashevsky, S. Fire-Retardant Action of Resorcinol Bis(diphenyl phosphate) in PC-ABS Blend. II. Reactions in the Condensed Phase. *J. Appl. Polym. Sci.* **1999**, *71*, 1863–1872.
- (25) Eckel, T.; Zobel, M.; Keller, B.; Wittmann, D. U.S. Patent 6 590 015, 2003.
- (26) Eckel, T.; Seidel, A.; Wittmann, D.; Peuker, U. U.S. Patent 6 316 579, 2003.
- (27) Wightman, R. H.; Malalyandi, M. Physical Properties of Some Synthetic Trialkyl/Aryl Phosphates Commonly Found in Environmental Samples. *Environ. Sci. Technol.* **1983**, *17*, 256–261.
- (28) T. D., N.; Suter, U. W. Detailed Molecular Structure of a Vinyl Polymer Glass. *Macromolecules* **1985**, *18*, 1467–1478.
- (29) Sun, H.; Ren, F. J.; Ren, P. The COMPASS Force Field: Parameterization and Validation for Phosphazenes. *Comput. Theor. Polym. Sci.* **1998**, *8*, 229–246.
- (30) Bunte, S. W.; Sun, H. J. Molecular Modeling of Energetic Materials: The Parameterization and Validation of Nitrate Esters in the COMPASS Force Field. *J. Phys. Chem. B* **2000**, *104*, 2477–2489.
- (31) Yang, J.; Ren, Y.; Tian, A.-M.; Sun, H. COMPASS Force Field for 14 Inorganic Molecules, He, Ne, Ar, Kr, Xe,  $\text{H}_2$ ,  $\text{O}_2$ ,  $\text{N}_2$ , NO, CO,  $\text{CO}_2$ ,  $\text{NO}_2$ ,  $\text{CS}_2$ , and  $\text{SO}_2$ , in Liquid Phases. *J. Phys. Chem. B* **2000**, *104*, 4951–4957.
- (32) Sun, H. COMPASS: An Ab Initio Force-Field Optimized for Condensed-Phase Applications—Overview with Details on Alkane and Benzene Compounds. *J. Phys. Chem. B* **1998**, *102*, 7338–7364.
- (33) Phillips, J. C.; Braun, R.; Wang, W.; Gumbart, J.; Tajkhorshid, E.; Villa, E.; Chipot, C.; Skeel, R. D.; Kale, L.; Schulten, K. Scalable Molecular Dynamics with NAMD. *J. Comput. Chem.* **2005**, *26*, 1781–1802.
- (34) Klauda, J. B.; Brooks, B. R.; MacKerell, A. D., Jr.; Venable, R. M.; Pastor, R. W. An Ab Initio Study on the Torsional Surface of Alkanes and Its Effect on Molecular Simulations of Alkanes and a DPPC Bilayer. *J. Phys. Chem. B* **2005**, *109*, 5300–5311.
- (35) Whitney, D. R.; Yaris, R. Local Mechanism of Phenyl Ring  $\pi$ -Flips in Glassy Polycarbonate. *Macromolecules* **1997**, *30*, 1741–1751.
- (36) Barnett, H. A.; Ham, K.; Butler, L. G. Synchrotron X-ray Tomography for 3D Chemical Diffusion Measurement of a Flame Retardant in Polystyrene. *Nucl. Instrum. Methods Phys. Res., Sect. A* **2007**, *582*, 202–204.
- (37) Li, X.-M.; Yang, R.-J. Study on Blooming of Tetrabromobisphenol A Bis(2,3-dibromopropyl ether) in Blends with Polypropylene. *J. Appl. Polym. Sci.* **2006**, *101*, 20–24.
- (38) Chen, Y.; Wang, Q. Thermal Oxidative Degradation Kinetics of Flame-Retarded Polypropylene with Intumescent Flame-Retardant Master Batches in Situ Prepared in Twin-Screw Extruder. *Polym. Degrad. Stab.* **2007**, *92*, 280–291.
- (39) Politou, A. S.; Morterra, C.; Low, M. J. D. Infrared Studies of Carbons. XII The Formation of Chars from a Polycarbonate. *Carbon* **1990**, *28*, 529–538.
- (40) Davis, A.; Golden, J. H. The Application of Gas Chromatography to the Characterisation and Thermal Degradation of a Polycarbonate. *J. Gas Chromatogr.* **1967**, *5*, 81–85.

(41) Davis, A.; Golden, J. H. Thermally-Induced Cross-Linking of Poly[2,2-propane-bis-(4-phenyl carbonate)]. *Macromol. Chem. Phys.* **1967**, *110*, 180–184.